Effect of particle size on the ferroelectric behaviour of tetragonal and rhombohedral $Pb(Zr_xTi_{1-x})O_3$ ceramics and powders

1995 J. Phys.: Condens. Matter 7 9287

(http://iopscience.iop.org/0953-8984/7/48/018)

J. Phys.: Condens. Matter 7 (1995) 9287–9303. Printed in the UK

Effect of particle size on the ferroelectric behaviour of tetragonal and rhombohedral $Pb(Zr_xTi_{1-x})O_3$ ceramics and powders

S K Mishra and Dhananjai Pandey

School of Materials Science and Technology, Banaras Hindu University, Varanasi-221 005, India

Received 16 March 1995, in final form 14 July 1995

Abstract. The effect of particle size on the structure and ferroelectric behaviour of PZT powders and ceramics with bulk tetragonal and rhombohedral compositions is reported. To our knowledge, this is the first report of particle size effects for the rhombohedral PZT composition. It is pointed out that, below a certain critical size, the formation of ferroelectric domains is not energetically favourable. As a result, the ferroelectric transition may be suppressed due to depolarization and/or elastic energy contributions.

1. Introduction

The effect of particle size on the ferroelectric transition in perovskites has received considerable attention in recent years [1–7] although the phenomenon has been known [8] for four decades. Investigation on particle size effects can be broadly classified into three categories: studies on firstly fine powders with free surfaces [1–8], secondly fine-grained ceramics with constrained grain surfaces [6, 9–17] and thirdly thin films [18]. Recent Raman scattering studies on fine powders of $PbTiO_3$ have revealed [1] that the transition temperature, as determined from the temperature dependence of the soft mode frequency, starts to decrease drastically for particle sizes below 50 nm ($\Delta T = T_c^{bulk} - T_c^{small} \leqslant 75\,^{\circ}C$). For particle sizes below 25 nm, the soft mode disappears, signalling the disappearance of the ferroelectric phase transition. The heat ΔQ of transition also decreases with decreasing particle size, indicating a decrease in the magnitude of the order parameter [3]. Below about 22 nm size, ΔQ almost vanishes, which implies suppression of the phase transition. High-temperature XRD studies on fine $BaTiO_3$ powders have also revealed [2] the lowering of T_c with decreasing particle size and eventual disappearance of the phase transition below about 120 nm size. All these recent findings on $PbTiO_3$ and $BaTiO_3$ particles are, however, contradictory to the earlier work of Kanzig and co-workers [8] who showed that for fine particles of $BaTiO_3$, obtained by mechanical ball milling as against chemical routes employed in recent investigations, T_c increases with decreasing particle size due to locked-in surface polarization.

Apart from the early work of Känzig and coworkers [8], a consistent picture has emerged over the recent years about the role of particle size in the ferroelectric transition in powder specimens. This is not so for ceramic and thin-film samples for which there are several contradictory reports. Kinoshita and Yamaji [11] reported a very small (2 °C or less) decrease in T_c with decreasing grain size for $BaTiO_3$ ceramics. Arlt *et al* [12] have shown that

0953-8984/95/489287+17$19.50

T_c initially increases with decreasing grain size but subsequently starts to decrease with decreasing grain size. An inspection of the ϵ' versus T plot reported by Vivekanandan *et al* [13] on the other hand does not reveal any change in T_c with decreasing grain size. The work of Martirena and Burfoot and of Yamamoto *et al* [10] on PZT ceramics and that of Okazaki and Nagata [9] on PLZT ceramics seems to suggest a significant increase in T_c with decreasing grain size. Scott *et al* [19] have noted that some of their thin-film specimens of PZT exhibit an increase in T_c with increasing grain size while others show a decrease. T_c for thin films of TGS, on the other hand, is found [20] to decrease with decreasing film thickness. Notwithstanding the conflicting reports on T_c, the ϵ' versus T plots in all the investigations on ceramics show smearing of the transition with decreasing grain size. The smearing of the ϵ' versus T plots has been correlated with structure in $BaTiO_3$ ceramics [12, 17]. No such report exists for PZT ceramics.

In the present work, we have studied the effect of particle size on the structure and ferroelectric behaviour of $Pb(Zr_xTi_{1-x})O_3$ (PZT) powders and ceramics. We have recently shown that the bulk structure of PZT ceramics prepared by a semiwet route is tetragonal for $x \leqslant 0.52$ while it is rhombohedral for $x \geqslant 0.53$ [21]. Here, it is shown that for both tetragonal and rhombohedral compositions,

(i) the ferroelectric transition is suppressed below a certain critical size, which is different for calcined powders and sintered ceramics,

(ii) the transition temperature T_c corresponding to the maximum value of the dielectric constant of the ceramics does not change within $\pm 1\,^{\circ}C$ with decreasing grain size and

(ii) maximum smearing of the ϵ' versus T plots is observed when the tetragonal or rhombohedral distortions are not discernible on XRD patterns of powders obtained after crushing the ceramic pellets.

Our results contradict the earlier observations of Martirena and Burfoot [10] on tetragonal PZT ceramics where T_c was shown to increase with decreasing grain size. In addition, we correlate the structural change, dielectric response and grain size. Further, to our knowledge, the present work is the first report of the particle size effect on rhombohedral PZT ceramics. The experimental observations are discussed in the light of the current explanations for grain size and particle size effects in ferroelectrics.

2. Experimental details

2.1. Powder synthesis

Ultrafine powders of PZT were synthesized by a semiwet route developed [21] in our laboratory. In this method, one first synthesizes a precursor hydroxide $(Zr_xTi_{1-x})(OH)_4$ by chemical coprecipitation. This hydroxide on thermal decomposition at 900 °C for 3 h yields a solid solution $(Zr_xTi_{1-x})O_2$. The oxide solid solution precursor is then ball milled with $PbCO_3$ for 6 h using zirconia balls and acetone as mixing media. As shown in [21], this mixture on calcination for 6 h at a temperature as low as 600 °C can yield single-phase fine powders of PZT. The reaction is faster at 700 °C as one can obtain single-phase PZT powders within 2 h of heat treatment. The powders used in the present work were calcined at 700 °C for 6 h to ensure completion of the reaction.

2.2. Sintering

Powders prepared at 700 °C were cold pressed using a die of 13.5 mm diameter at a uniaxial load of 100 kN using 2% PVA solution as a binder. The green pellets were fired at

500 °C for 10 h to burn off PVA. Pellets so obtained were then sintered at 700, 900, 1000, 1100 and 1200 °C for 6 h for the composition with $x = 0.52$. For the composition with $x = 0.535$, sintering was performed at 700, 900, 1000 and 1050 °C for 6 h. Higher sintering temperatures for $x = 0.535$ led to partial melting. The loss of PbO during sintering was controlled by performing the sintering in the presence of $PbZrO_3$ powders to maintain sufficient PbO vapour pressure inside MgO-sealed alumina crucibles. In this way, we were able to control the PbO loss without adding excess of $PbCO_3$ to the initial composition. The representative sintered densities and percentage weight loss for each batch of sintering are given in table 1. It is evident from this table that the weight loss in the pellets due to the possible escape of PbO at high temperatures is quite small. Further, with increasing sintering temperature, the bulk density of the pellets increases.

2.3. Microstructure and crystal structure

By varying the sintering temperature, it was possible to vary the grain size. The grain size was measured using optical and scanning electron micrographs obtained from polished and chemically etched (2% HF solution in HCl) specimens. XRD patterns of as-calcined and sintered materials were recorded on a rotating-anode Rigaku powder diffractometer operating at 50 kV and 120 mA.

2.4. Dielectric measurements

The dielectric constant was measured at 10 and 100 kHz using a Schulemberger impedance–gain phase analyser model 1260. Fired-on silver electrodes (firing temperature, 500 °C) were applied on the surface of the pellets after it was gently polished with 0.25 μm diamond paste. The temperature was controlled to within ± 1 °C using a programmable temperature controller. The dielectric measurements were performed at a heating rate of 1 °C min^{-1}. It was verified that the lower heating rate did not affect T_c.

3. Results

3.1. Variation in grain size with sintering temperature

The particle size of the as-calcined powders for both the compositions is less than 0.1 μm (see [21]). Sintering of these powders at 500 and 700 °C did not change the particle size of the as-calcined powders. Grain growth was observed for samples sintered at 900 °C and above. Figures 1 and 2 depict the microstructures of tetragonal $Pb(Zr_{0.52}Ti_{0.48})O_3$ and rhombohedral $Pb(Zr_{0.535}Ti_{0.465})O_3$ compositions after sintering at different temperatures. The average grain sizes of the ceramics corresponding to the tetragonal composition ($x = 0.52$) are found to be 0.6 μm, 2.6 μm, 4.2 μm and 4.8 μm after sintering at 900 °C, 1000 °C, 1100 °C and 1200 °C, respectively. For the samples sintered at 900 °C, the grain size was obtained from regions were PZT material had peeled off during polishing. All the microstructures except for the 1000 °C sintering cycle were obtained using SEM. The microstructure of the 1000 °C-sintered specimen was obtained using optical microscopy. For the rhombohedral composition ($x = 0.535$), the average grain sizes are 0.6 μm, 2.3 μm and 4.5 μm after sintering at 900 °C, 1000 °C and 1050 °C, respectively. All these micrographs were taken using SEM.

Table 1. Sintered densities and percentage PbO losses during sintering at various temperatures.

Composition (x)	Sintering temperature (°C)	Sintered density (g cm^{-3})	Weight loss (%)
0.520	500	6.12	0.003
	700	6.35	0.011
	900	6.44	0.056
	1000	7.60	0.374
	1100	7.72	0.041
	1200	7.76	0.015
0.535	500	6.12	0.047
	700	7.21	0.061
	900	7.40	0.009
	1000	7.59	0.056
	1050	8.03	0.034

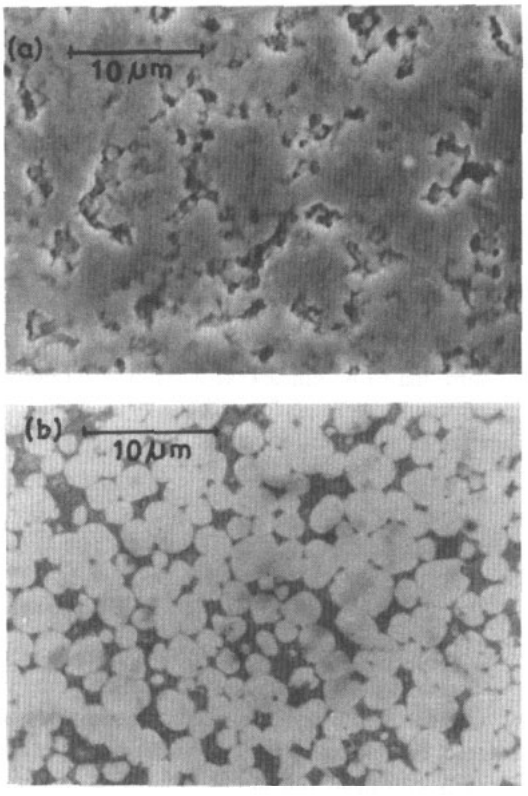

Figure 1. Optical and scanning electron micrographs of tetragonal $Pb(Zr_{0.520}Ti_{0.480})O_3$ ceramics sintered at different temperatures: (*a*) 900 °C (SEM); (*b*) 1000 °C; (*c*) 1100 °C (SEM); (*d*) 1200 °C (SEM).

3.2. Variation in crystal structure with grain size

The effect of particle size on the crystal structure of PZT was studied using 111 and 200 reflections of the cubic perovskite phase. For the tetragonal structure, the 200 reflection is a doublet while 111 is a singlet. For the rhombohedral phase of PZT, the 111 is a doublet

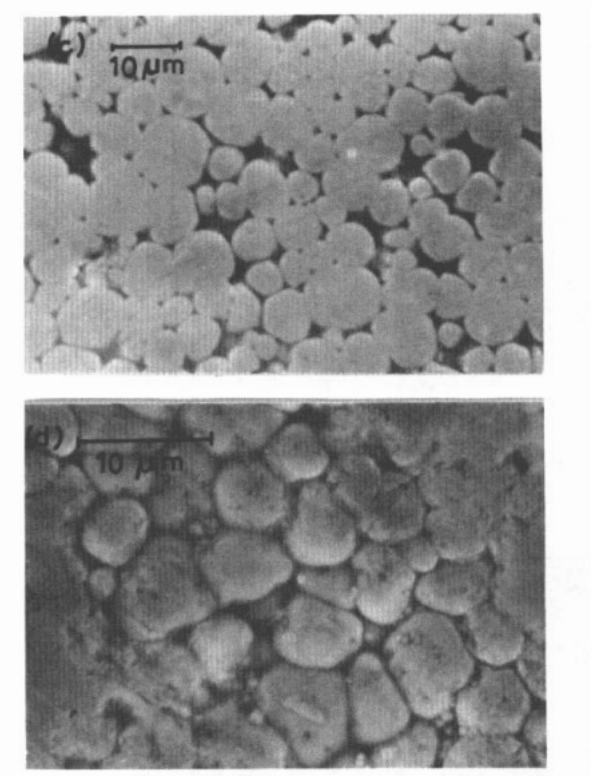

Figure 1. (Continued)

consisting of $11\bar{1}$ and 111 reflections while 200 remains a singlet.

Figure 3 depicts the XRD patterns of the as-calcined powders obtained at 700 °C for $x = 0.52$ and 0.535. From these diffractograms, the structures of both the powders at this stage appear to be cubic. Figure 4 depicts the XRD profiles for the 111 and 200–002 reflections after sintering at 500, 700, 900, 1000, 1100 and 1200 °C for $x = 0.52$. Sintering at 500 and 700 °C does not change either the grain size or the structure, i.e. the structure remains cubic. The sample sintered at 900 °C shows a tail on the small-angle side which may be attributed to the onset of separation of the 002 reflection from the 200–020 reflections due to the appearance of the tetragonal distortion. Sintering at temperatures higher than 900 °C makes the grains large enough to exhibit the tetragonal distortion clearly. The resolution of the 002 and 200–020 reflections gradually improves with increasing sintering temperature, which in turn leads to larger grain sizes.

A similar behaviour is observed for the rhombohedral composition ($x = 0.535$). The XRD profiles of samples with this composition sintered at different temperatures are given in figure 5. Here also, the rhombohedral distortion, as revealed by the appearance of 111 and $11\bar{1}$ reflections, becomes discernible in samples sintered at temperatures of 900 °C or higher. The structure of samples sintered below 900 °C remains essentially cubic.

Correlating the structural distortion with grain size discussed in the previous section, it may be concluded that the tetragonal–rhombohedral distortions are discernible for grain sizes approximately equal to or higher than about 0.5 μm. Also these distortions increase with increasing grain size.

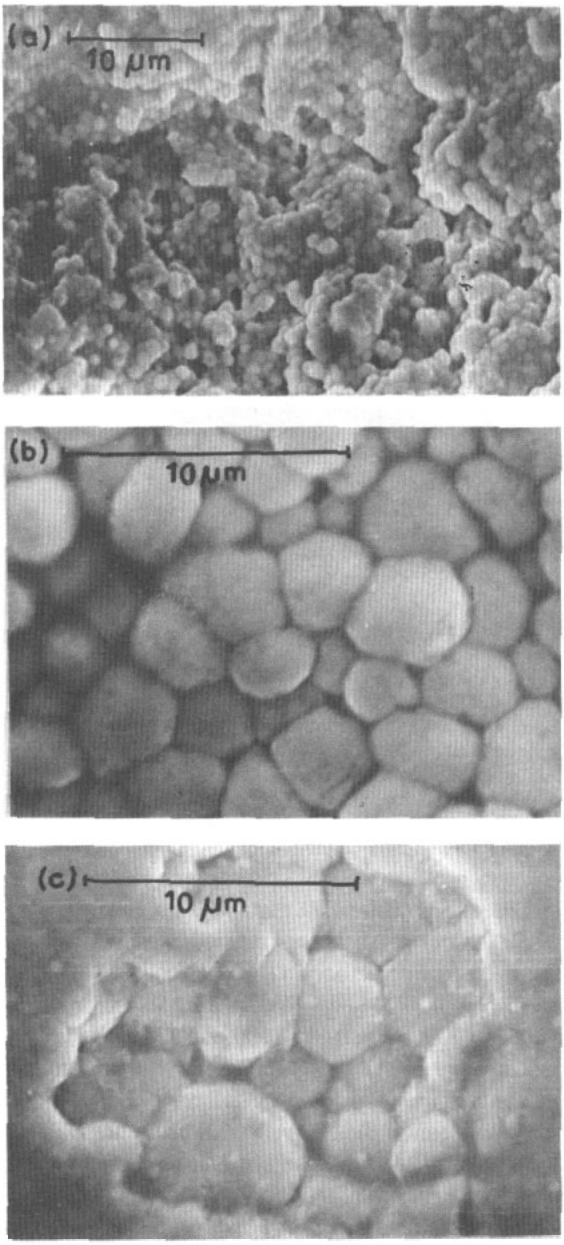

Figure 2. Scanning electron micrographs of rhombohedral $Pb(Zr_{0.535}Ti_{0.465})O_3$ ceramics sintered at different temperatures: (*a*) 900 °C; (*b*) 1000 °C; (*c*) 1050 °C.

3.3. Temperature dependence of dielectric constant

The temperature variation in the real part ϵ' and the imaginary part ϵ'' of the dielectric constant for the tetragonal and rhombohedral compositions for specimens of different grain sizes are shown in figures 6–9 at 10 and 100 kHz measurement frequencies. There are several notable features in these figures.

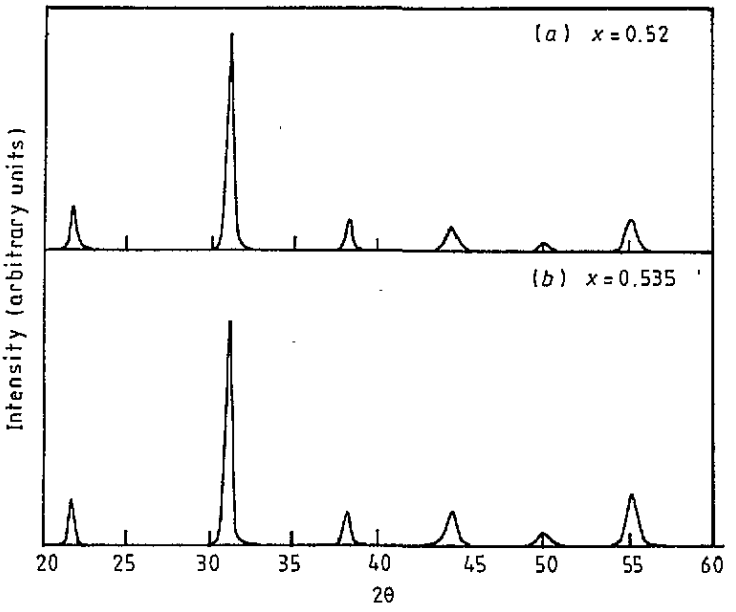

Figure 3. XRD pattern of the as-calcined powders of $Pb(Zr_xTi_{1-x})O_3$ obtained at 700 °C: (*a*) for $x = 0.520$; (*b*) for $x = 0.535$.

(a) The samples sintered at 500 °C do not exhibit any dielectric anomaly whereas those sintered at 700 °C exhibit an anomaly, although quite weak for the tetragonal composition. As stated earlier, both the samples have a cubic structure at the XRD level and their grain sizes are comparable.

(b) The smearing or diffuseness of the phase transition for ϵ' versus T plots decreases with increasing sintering temperature (900 °C onwards) and hence increasing grain size and tetragonal–rhombohedral distortion.

(c) The temperature at which ϵ' peaks does not change with grain size within the accuracy of the measurement of temperature (±1 °C).

(d) Although the absolute values of ϵ' change with frequency, the transition temperature remains unaffected on increasing the measurement frequency from 10 to 100 kHz.

(e) The dielectric loss (ϵ'') peaks also occur at the same temperature at which ϵ' peaks. This is quite clear for the 100 kHz measurement although, at temperatures above T_c, ϵ'' again starts to rise, presumably due to the rising trend of conductivity. The conductivity losses are more pronounced at the lower frequency (10 kHz), masking the ϵ'' peak at T_c partly (see inset of figure 6) or fully (see inset of figure 8). It is interesting to note that this effect is less pronounced for samples with smaller grain sizes due to their lower densities or high porosities which in turn influence the conductivity due to poor grain connectivity. It is interesting to note that the grain size independence of T_c for $x = 0.535$ is better seen in the ϵ'' versus T plot shown as an inset on figure 9 than in the ϵ' versus T plot for samples sintered at $T \geqslant 900$ °C.

(f) For the rhombohedral composition, the room-temperature dielectric constant of samples sintered at 700 °C is higher than that of those sintered at 900 °C even though the density of higher-temperature-sintered ceramic is higher (see figure 9). If one applies the density correction in the manner described in [24], this difference in dielectric constant becomes even larger. This indicates that, with decreasing grain size or rhombohedral

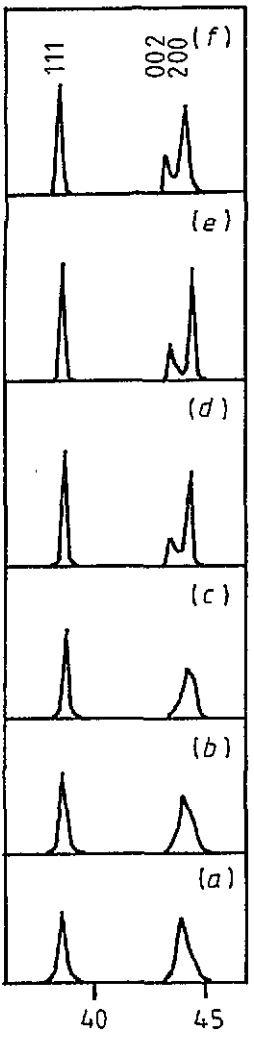

Figure 4. XRD profiles for 111, 200 and 002 reflections for $x = 0.52$ after sintering at (*a*) 500 °C, (*b*) 700 °C, (*c*) 900 °C, (*d*) 1000 °C, (*e*) 1100 °C and (*f*) 1200 °C.

distortion, the value of dielectric constant may pass through a maximum as has been reported for $BaTiO_3$ [12, 17].

3.4. X-ray line broadening analysis of calcined and sintered powders

The XRD profiles in figure 3 for as-calcined powders are considerably broadened for both the compositions. In this situation, it is necessary to decide whether the profiles are due to a truly cubic structure or contain inhomogeneous lattice distortions masked by the particle size broadening. It is possible to distinguish between particle size and strain-broadening effects by analysing the line broadening of the XRD profiles. As explained in [22], in a plot of $\beta \cos\theta$ versus $\sin\theta$ for different reflections, where β is the FWHM of the true diffraction profile and θ the Bragg angle, one expects a straight line with a zero slope for pure particle size broadening. A non-zero slope of the straight line indicates the presence of strains caused by inhomogeneous lattice distortions and/or compositional inhomogeneities. Figures 10 and 11 depict the $\beta \cos\theta$ versus $\sin\theta$ plots for the as-calcined powders with $x = 0.535$ and 0.520

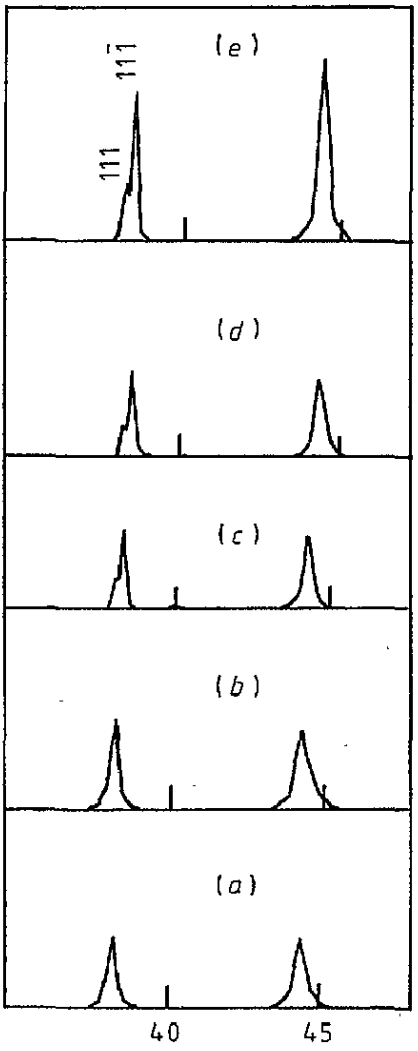

Figure 5. XRD profiles for 111, 11$\bar{1}$ and 200 reflections for $x = 0.535$ after sintering at (*a*) 500 °C, (*b*) 700 °C, (*c*) 900 °C, (*d*) 1000 °C and (*e*) 1050 °C.

prepared at 700 °C. It is evident from these figures that the data points fall on horizontal lines as expected for pure particle size broadening, ruling out the possibility of inhomogeneous strains due to spatial variation of lattice distortions. We would, however, like to add that the possibility of the presence of lattice distortions well below the resolution limit $\Delta d/d$ of the diffractometer cannot be ruled out. As such, powders may not be truly cubic but only pseudo-cubic, containing mosaic-like local distortions. The fact that one observes a hump in the ϵ' versus T plots for samples sintered at 700 °C, which is low enough to cause grain growth with respect to the size of the particles in the as-calcined powders, suggests the presence of polar clusters and hence a pseudo-cubic structure. For a truly cubic structure, one does not expect any dielectric anomaly as a function of temperature.

For the sintered specimens, it was shown in the previous section that with increasing grain size the tetragonal and/or rhombohedral distortions increase. Concomitantly, the

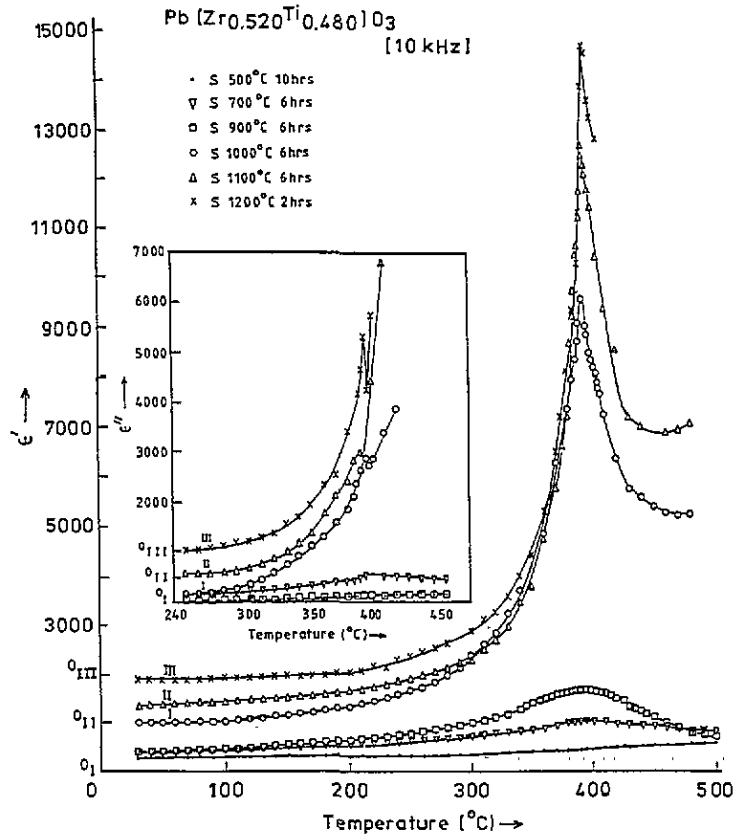

Figure 6. Temperature dependence of the dielectric constant measured at 10 kHz of $Pb(Zr_{0.520}Ti_{0.480})O_3$ ceramics sintered at 500, 700, 900, 1000, 1100 and 1200 °C.

dielectric constant versus temperature curves also sharpen. Since sintering can influence the crystallinity of the grains, it is important to determine the coherently scattering domain size of the sintered specimen as a function of sintering temperature [23]. Table 2 gives the coherently scattering domain size as determined using the Scherrer equation for the broadening of 111 and 110 reflections of the tetragonal and rhombohedral compositions as a function of sintering temperature. The results of sintering at 500 °C were similar to those for sintering at 700 °C. It is evident from this table that, for the rhombohedral composition, the coherently scattering domain size remains almost constant irrespective of the sintering temperature. For the tetragonal composition, there seems to be a slight increase in the coherently scattering domain size with increasing sintering temperature except for 1200 °C. However, the fact that the coherently scattering domain sizes for samples sintered at 900 and 1200 °C are identical suggests that the variations with sintering temperature may not be significant compared with the accuracy of the analysis. Keeping in mind the errors in firstly the deconvolution procedure for obtaining the FWHM of the true diffraction profile from measured profiles and secondly the separation of the $K\alpha_2$ contribution using the Rachinger method, the uncertainty in $\overline{D}$ can be quite large. The results for rhombohedral composition, however, clearly rule out any change in the coherently scattering domain size as a function of sintering temperature. Hence the effects described in the previous sections are purely a grain size effect.

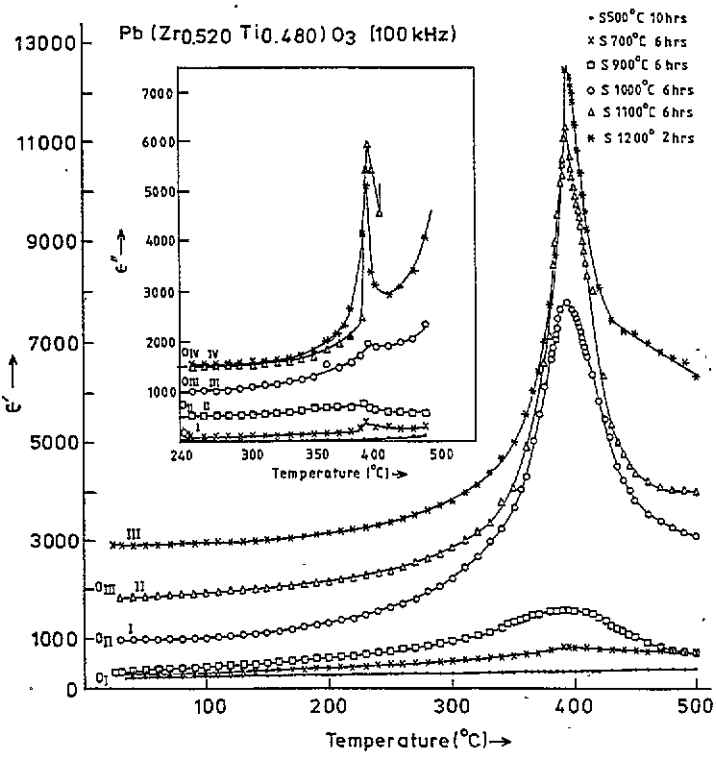

Figure 7. Temperature dependence of the dielectric constant measured at 100 kHz of $Pb(Zr_{0.520}Ti_{0.480})O_3$ ceramics sintered at 500, 700, 900, 1000, 1100 and 1200 °C.

Table 2. Coherently scattering domain sizes in samples sintered at different temperatures.

Composition (x)	Sintering temperature (°C)	Domain size (Å)
0.520	700	617
	900	744
	1000	767
	1100	834
	1200	744
0.535	700	529
	900	547
	1000	540
	1050	550

4. Discussion

We shall compare our results with those reported for $BaTiO_3$ ceramics where grain size effects have been investigated in great detail. There are two different types of grain size effect in $BaTiO_3$ ceramics.

(i) The room-temperature dielectric constant of $BaTiO_3$ ceramics exhibits a maximum value for grain sizes in the range 0.4–0.8 μm [12, 25]. The name 'size-driven phase transition' has been coined for this phenomenon [26].

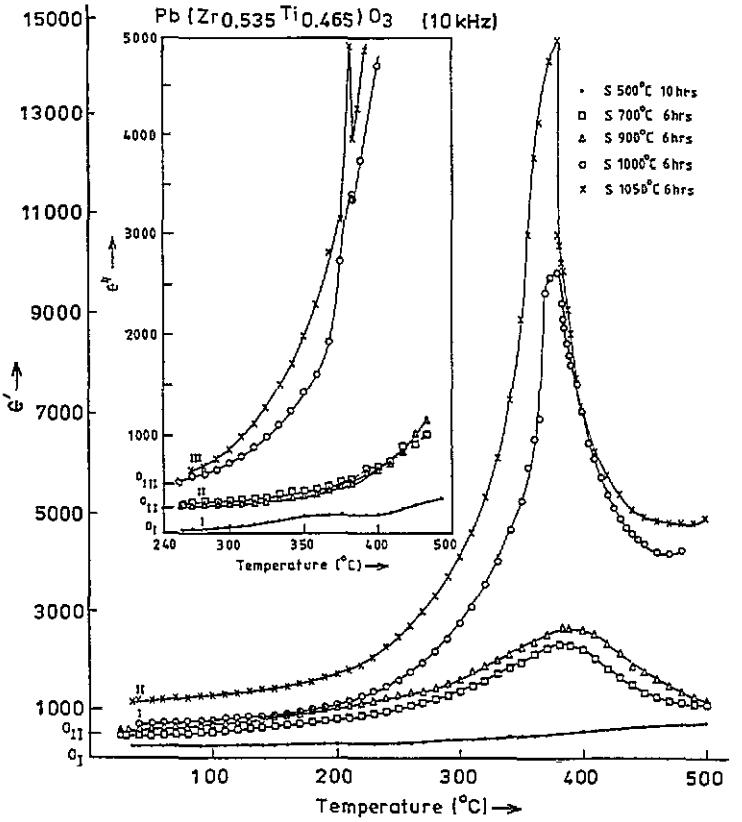

Figure 8. Temperature dependence of the dielectric constant measured at 10 kHz of $Pb(Zr_{0.535}Ti_{0.465})O_3$ ceramics sintered at 500, 700, 900, 1000 and 1050 °C.

(ii) The transition from the cubic paraelectric phase to the tetragonal ferroelectric state appears diffuse on ϵ' versus T plots with the suppression of the peak value of the dielectric constant in fine-grained ceramics.

Early attempts to understand the two types of grain size effect in $BaTiO_3$ ceramics were based on an internal stress model [27–29]. When $BaTiO_3$ ceramics are cooled through the ferroelectric transition temperature, the external constraints due to adhering grains do not allow for development of full transformation strains since it requires gross motion of the grain surfaces. The formation of 90° domains for the cubic-to-tetragonal transition usually helps to relieve these strains in large-grained ceramics. It has been argued [27] that, if the grain size becomes comparable to the width of 90° domain walls, such domains cannot be formed. Around this critical size, the grains are expected to be of a single-domain nature and may be subjected to a complex stress distribution due to the unrelieved transformation strains. These internal stresses were believed [27] to be responsible for the increase in the room-temperature dielectric constant of $BaTiO_3$ ceramics with grains of less than 1 μm size. Micheron [28] attempted to explain the diffuseness of the dielectric transition in fine-grained $BaTiO_3$ ceramics as being due to a distribution of transition temperatures in different grains because they were subjected to a distribution of internal stresses. The near absence of 90° domains in grains of less than 1 μm size in optical microscopy observations was taken as one piece of evidence in support of the internal stress model. The internal stress model

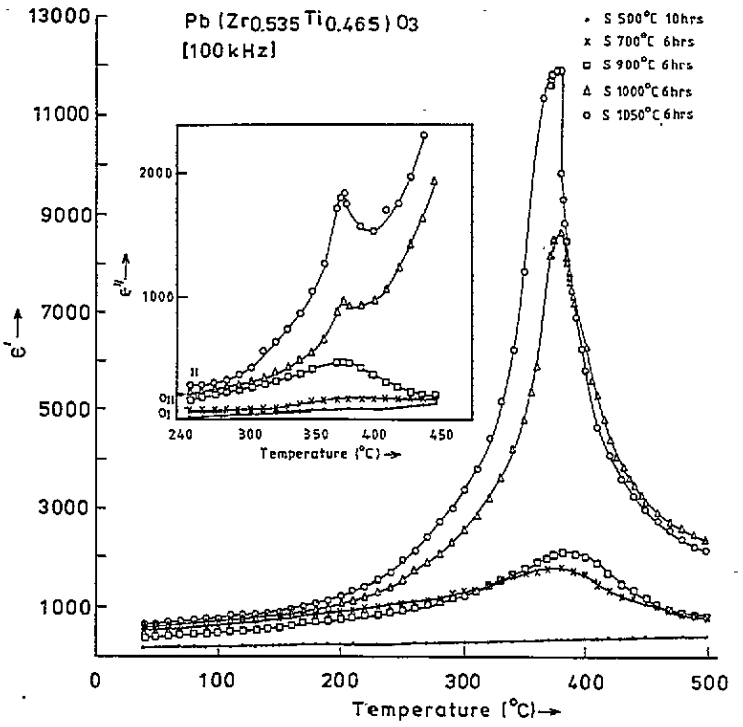

Figure 9. Temperature dependence of the dielectric constant measured at 100 kHz of $Pb(Zr_{0.535}Ti_{0.465})O_3$ ceramics sintered at 500, 700, 900, 1000 and 1050 °C.

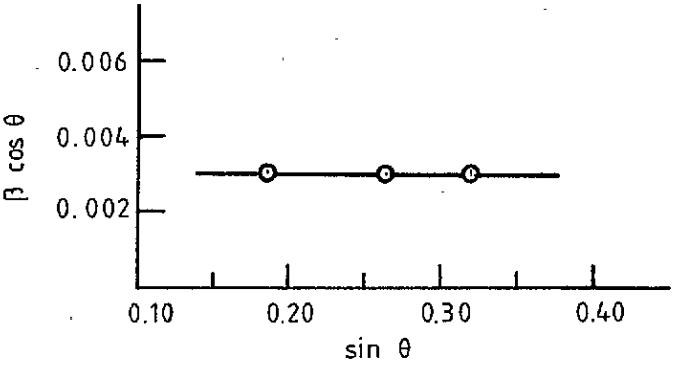

Figure 10. $\beta \cos\theta$ versus $\sin\theta$ plots for the as-calcined powders with $x = 0.520$.

has in recent years been questioned in the light of the observation of 90° domain walls in grains as small as 0.5 μm using SEM and TEM techniques [12]. Using high-resolution electron microscopy techniques, the 90° walls have been shown to be fairly sharp and restricted to a few tens of ångströms only [30]. It has been proposed [12] that the higher dielectric constant in fine-grained $BaTiO_3$ ceramics may be due to an increased contribution from the domain wall to the total dielectric constant on decreasing the grain size. Since the orthorhombic-to-tetragonal transition temperature in $BaTiO_3$ is raised considerably with decreasing grain size, the higher value of dielectric constant at room temperature in fine-

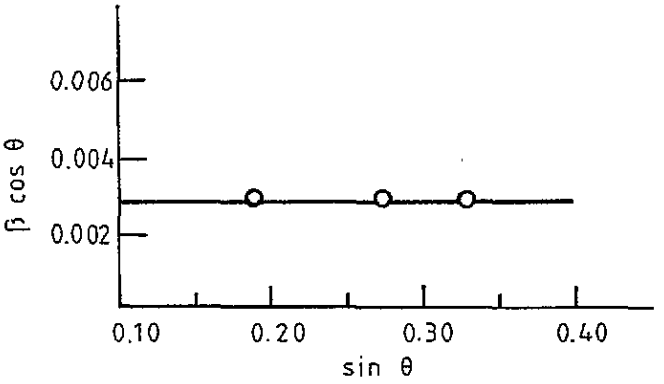

Figure 11. $\beta \cos\theta$ versus $\sin\theta$ plots for the as-calcined powders with $x = 0.535$.

grained $BaTiO_3$ ceramics can also be attributed to the rising trend of ϵ' in the vicinity of the tetragonal-to-orthorhombic phase transition.

The last possibility is clearly ruled out in the PZT system where there is no phase transition below room temperature, and still the room-temperature dielectric constant for the smaller-grain-size sample obtained after sintering at 700 °C is grater than that of larger-grain-size samples sintered at 900 °C for the 0.535 series (see figure 9). This enhancement of dielectric constant with decreasing grain size in PZT cannot be attributed to internal stresses either, since in PZT the structure of the ceramic specimens sintered at 700 °C is essentially cubic in both powder and sintered forms at the XRD level. Internal stresses may be deemed to be present in single-domain grains of ceramic specimens only if the structure of the grains is tetragonal at least in the powder form. By a similar token, the explanation [12] based on the increased contribution of 90° domain walls to the overall dielectric constant below a certain critical grain size does not seem to be applicable due to the absence of the cubic-to-tetragonal phase transition at the XRD level. Fresh insight is therefore needed to understand these size-dependent phenomena.

It is well known that an ideally sharp transition can occur in the thermodynamic limit of infinite system size. For real finite-size systems, phase transitions are rounded and shifted with different characteristic exponents for the first- and second-order phase transitions [31]. Even in finite-size systems, the phase transition behaviour changes drastically as one moves from the larger end of the size spectrum towards the smaller end due to the increasingly important role of the surface which no longer remains negligible compared to the bulk volume. When an insulating crystal undergoes a paraelectric-to-ferroelectric phase transition in the absence of an external electric field, it splits into domains of uniform polarization to compensate for the depolarization field due to the uncompensated charges on the surface [6]. The equilibrium domain width for simple lamellar geometry has been predicted on the basis of minimization of the appropriate Landau free-energy functional together with the depolarization and domain wall energy terms [32, 33]. Qualitative phenomenological considerations show that, below a certain critical size t_{crit}, it may not be possible to recover the wall energy term ($O(t^2)$) from the depolarization energy term ($O(t^3)$) [6, 33]. As a result of this, the uncompensated depolarization field may be intense enough to suppress the ferroelectric transition altogether [6, 33]. If the surface of the particle undergoing the ferroelectric transition is not free, as in ceramic grains, an elastic energy term ($O(t^3)$) may

also have to be taken into account in the energy balance. The magnitude of the depolarization as well as elastic energy terms will depend on the net lattice deformation or the order parameter $\overline{P}$ which has to be obtained from a self-consistent solution of the Landau-type free-energy functional together with the various other energy terms mentioned above [33]. When the size of the particles becomes comparable to the critical size mentioned above, one expects a single-domain particle below the transition temperature. For $BaTiO_3$ ceramics, the critical grain size for the destabilization of the ferroelectric state has been reported to be in the range 0.4–0.8 μm [12, 17]. For PZT ceramics, as per the results described in the previous section, this critical grain size seems to be around 0.6 μm. Somewhere below this grain size, the XRD pattern will start to show pseudo-cubic symmetry but may still continue to exhibit a pronounced hump in the temperature variation of dielectric constant. With further reduction in grain size approaching a few atomic dimensions, one expects the disappearance of this hump and the structure may become truly cubic. There is thus a second critical size which seems to be an order of magnitude smaller than the critical size at which single-domain particles or grains with substantially reduced tetragonality are observed. The hump in the ϵ' versus T plots for samples showing pseudo-cubic symmetry at the XRD level has to be attributed to cooperative dipolar clustering well below the detection limit of XRD. The dielectric behaviour of such fine-grained ceramics can be understood in terms of the fluctuating dipolar clusters which can be frozen by a relatively weak electric field at a suitably low temperature. The situation appears similar to the high responsiveness of the superparamagnetic state and can be termed a superparaelectric state [34] in the present context. The relaxation time of the fluctuating dipolar clusters seems to be either too large or too small compared to the time period of the alternating field to lead to frequency dependence of the ϵ' and ϵ'' peak temperatures at 10 and 100 kHz. Very-low-frequency as well as high-frequency measurements are required to settle this proposition in any future study.

The ceramics prepared from the as-calcined powders of $Pb(Zr_{0.52}Ti_{0.48})O_3$ with size less than 0.1 μm [21] on sintering at 700 °C (which is low enough to cause any grain growth) exhibit a hump in the temperature variation of the dielectric constant. On the other hand, ceramics obtained from the same powders but sintered at 500 °C did not exhibit any dielectric anomaly in the ϵ' versus T plots although the grain size for these ceramics are comparable to those of that sintered at 700 °C. This is because of the high porosity and lack of chemical bonding between the grains at such lower sintering temperatures. As a result of these, the continuity of the electric flux from grain to grain is not achieved at all, which in turn masks the dielectric anomaly near the transition temperature [24]. The difference between the behaviours of ceramics sintered at different temperatures cannot be attributed to improved coherently scattering domain size [23] since it does not change with sintering temperature, as already shown in section 3.4.

A drastic drop in the transition temperature, as investigated by Raman scattering [1], specific heat [3] and high-temperature XRD [2] studies, seems to occur around the critical size at which the ferroelectric state first becomes destabilized due to the absence of domain structure. A qualitative microscopic understanding of this decrease in T_c has been proposed [1, 3, 6] within the soft-mode theory of the ferroelectric transition of displacive type. The freezing of the soft mode in displacive ferroelectrics depends on the cancellation of short-range forces by long-range Coulombic forces. The latter depends on the Lorentz field E_s due to dipole summation and the depolarization field E_d. In an infinite system size, $E_d = 0$ and E_s is large enough to lead to the cancellation of short-range forces at the transition temperature. As the system size decreases, the dipole summation runs over a limited volume, and $E_d \neq 0$ due to the absence of domains. As a result, the cancellation of the short- and

long-range forces occurs at a lower temperature at which the contribution of the short-range term itself is reduced. However, with continued reduction in size, the E_s term may become too small to lead to the cancellation of the short-range forces. This is expected to occur at the second critical size discussed in the previous paragraph.

In a ceramic sample, there will always be a distribution of grain sizes. As the grain size decreases, one expects the size of some of the grains to lie between the two critical sizes. These grains will therefore possess T_c-values which are much lower than the bulk T_c. As a result of this, the sharp change in the dielectric constant at T_c will be replaced by a more sloppy or diffuse behaviour with an increasing number of grains having sizes smaller than the first critical size. Depending on the number density and volume fraction of such small grains compared to the larger grains, the transition would become more and more diffuse and the identification of the dielectric constant peak temperature with a single phase transition temperature T_c loses its significance. Thus the observed diffuseness of the ϵ' versus T plots as well as the shift of the dielectric hump temperature can be attributed to the distribution of transition temperatures for individual grains whose size is below the first critical size. If more grains have sizes below this critical value, the hump temperature may shift to a lower value. The detection of such a shift will, however, be possible only if the hump is not flat over 5–10 °C. In our PZT samples, it is meaningless to look for such shifts since $d\epsilon/dT$ is nearly zero over a large temperature range near the hump temperature for samples sintered at 700 °C. While lowering of the hump temperature, as observed for $BaTiO_3$ ceramics [11], can be rationalized in terms of the picture presented above, there is no way that one can account for the increases in the hump temperature as reported by a few earlier workers [9, 10] for PLZT and PZT ceramics. It has been reported that uniaxial compressive stresses applied parallel to the electrode surface can raise the hump temperature [35]. Such a uniaxial stress may be introduced during lapping or polishing of the surface prior to the application of the fired-on electrodes [36]. To avoid these stresses, use of ultrafine diamond paste has been recommended [36]. It is likely that the higher hump temperatures reported for PLZT and PZT ceramics are due to such extrinsic factors which were ruled out in the present work by the use of 0.25 μm diamond paste as a polishing agent. Even the observation of Känzig and coworkers [8] about a higher T_c in fine $BaTiO_3$ powders obtained by mechanical milling may be due to the presence of the complex stresses introduced by the milling process.

5. Conclusions

(1) The cubic-to-tetragonal or rhombohedral phase transition is suppressed below a certain critical size in PZT particles due to the intense depolarization fields caused by the absence of ferroelectric domains.

(2) In sintered ceramics, both the depolarization field as well as the transformation strains may be responsible for the suppression of the phase transition.

(3) The observed diffuseness of the ϵ' versus T plots is due to the presence of such single-domain grains of different sizes with different T_c values.

Acknowledgments

Financial support from the Defence Research and Development Organisation is gratefully acknowledged. We also thank Professor V D Vankar for his help in taking SEM pictures.

References

[1] Ishikawa K 1988 *Phys. Rev.* B **37** 5852
[2] Uchino K, Sadanaga E and Hirose T 1989 *J. Am. Ceram. Soc.* **72** 1555
[3] Zhong W L, Jiang B, Zhang P L, Ma J M, Cheng H M, Yang Z H and Li L X 1993 *J. Phys.: Condens. Matter* **5** 2619
[4] Meng J, Zou G, Ciu Q, Zhao Y and Zhu Z 1994 *J. Phys.: Condens. Matter* **6** 6543
[5] Meng J, Zou G, Ma Y, Wang X and Zhao M 1994 *J. Phys.: Condens. Matter* **6** 6549
[6] Pandey D, Singh N and Mishra S K 1993 *Indian J. Pure Appl. Phys.* **32** 616
[7] Zhong W L, Wang Y G, Zhang P L and Qu B D 1994 *Phys. Rev.* B **50** 698
[8] Jaccard C, Känzig W and Peter M 1953 *Helv. Phys. Acta* **26** 52
Anliker M, Brugger H R and Känzig W 1954 *Helv. Phys. Acta* **27** 99
[9] Okazaki K and Nagata K 1973 *J. Am. Ceram. Soc.* **56** 82
[10] Martirena H T and Burfoot J C 1974 *J. Phys. C: Solid State Phys.* **7** 3182
Yamamoto T, Tanka R, Okazaki K and Ueyama T 1989 *Japan. J. Appl. Phys. Suppl.* **28-2** 63
[11] Kinoshita K and Yamaji A 1976 *J. Appl. Phys.* **47** 371
[12] Arlt G, Hennings D and deWith G 1985 *J. Appl. Phys.* **58** 1619
[13] Vivekanandan R, Philip S and Kutty T R N 1986 *Mater. Res. Bull.* **22** 99
[14] Kanata T, Yoshikawa T and Kubota K 1987 *Solid State Commun.* **62** 765
[15] Arlt G 1990 *Ferroelectrics* **104** 217
[16] Takenchi T, Ado K, Asai T, Kageyama H, Saito Y, Masquelier C and Nakamura O 1994 *J. Am. Ceram. Soc.* **77** 1665
[17] Perriat P, Niepce J C and Caboche G 1994 *J. Therm. Anal.* **41** 635
[18] Scott J F 1991 *Phase Trans.* **30** 107
[19] Scott J F, Duiker H M, Beale P D, Pouligny B, Dimmler K, Parris M, Butler D and Eaton S 1988 *Physica* B **150** 160
[20] Batra I P, Wurfel P and Silverman B D 1973 *Phys. Rev. Lett.* **30** 384
[21] Singh A P, Mishra S K, Pandey D, Durgaprasad Ch, Ramji L and Pandey D 1993 *J. Mater. Sci.* **28** 5050
[22] Tiwari V S, Singh N and Pandey D 1995 *J. Phys.: Condens. Matter* **7** 1441
[23] Criado J M, Dainez M J, Gotor F, Real C, Mundi M, Ramos S and Del Credo J 1992 *Ferroelectrics Lett.* **14** 79
[24] Gachigi K W, Kumar U and Dougherty J P 1993 *Ferroelectrics* **143** 229
[25] Shaikh A S, Vest R W and West G W 1989 *IEEE Trans. Ultrasonics, Ferroelectrics Frequency Control* **36** 407
[26] Multani M S and Ayyub P 1991 *Condens. Matter News* **1** 25
[27] Buessem W, Goswami A K and Cross L E 1966 *J. Am. Ceram. Soc.* **49** 33
[28] Micheron F 1972 *Rev. Tech. Thompson-CSF* **4** 5
[29] Bell A J 1993 *Ferroelectrics Lett.* **15** 133
[30] Demczyk B G, Rai R S and Thomas G 1990 *J. Am. Ceram. Soc.* **73** 615
[31] Binder K 1987 *Ferroelectrics* **73** 43
[32] Lines M E and Glass A M 1977 *Principles and Application of Ferroelectrics and Related Materials* (Oxford: Clarendon)
[33] Sharma P and Pandey D to be published
[34] Newnham R E, Mckinstry S E and Ikawa H 1990 *(Mater. Res. Soc. Symp. Proc. 175)* (Pittsburgh, PA: Materials Research Society) p 161
[35] Shirane G and Sato K 1951 *J. Phys. Soc. Japan* **6** 20
[36] Jyomura S, Matsuyama I and Toda G 1980 *J. Appl. Phys.* **51** 219